JOURNAL OF GEOPHYSICAL RESEARCH, VOL. 114, B11303, doi:10.1029/2009JB006288, 2009

Love wave dispersion in central North America determined using absolute displacement seismograms from high-rate GPS

James P. Davis[1] and Robert Smalley Jr.[1]

Received 31 December 2008; revised 6 July 2009; accepted 28 July 2009; published 3 November 2009.

[1] We use seismic array processing of high-rate GPS (HRGPS) displacement time series from the Great, 2004, M_w 9+, Sumatra-Andaman earthquake recorded at over 90 nonuniformly distributed HRGPS stations in central North America to determine the fundamental Love wave phase velocity dispersion curve there. These measurements were performed using frequency domain beam forming, which we show reduces the effects of GPS multipath and common mode noise on the measurement of surface wave phase velocity and azimuth. Our HRGPS based results for surface wave phase velocity agree well with those obtained from 28 broadband seismometers between periods of 20 to 300 s. By separating waves based on their apparent velocity, beam forming supports the simple model for relative displacement HRGPS time series as being the difference between the reference and kinematic station's absolute displacements. Beam forming also demonstrates that for differential GPS processing the infinite apparent velocity beam of an array is composed of the sum of common mode noise and the reference station's absolute displacements, multipath and noise. We show the infinite apparent velocity beam, which we call the generalized spatial filter, is similar to the spatial filter commonly used to remove common mode noise from HRGPS seismograms and can be used to produce absolute displacement time series for the kinematic stations with reduced common mode noise. Beam forming also suggests a filtering method, complimentary to sidereal filtering, to produce GPS multipath reduced HRGPS time series.

Citation: Davis, J. P., and R. Smalley Jr. (2009), Love wave dispersion in central North America determined using absolute displacement seismograms from high-rate GPS, *J. Geophys. Res.*, *114*, B11303, doi:10.1029/2009JB006288.

1. Introduction

[2] We apply seismic array processing analysis techniques to high-rate GPS (HRGPS) displacement time series to measure surface wave dispersion and investigate how array processing can improve HRGPS displacement seismograms. One significant result is that the spatial filter method, developed to remove common mode noise, can be generalized to also remove the reference station's contribution from differential GPS displacements to produce absolute GPS displacements. This is because the generalized spatial filter we introduce contains everything that is common mode, which beam forming demonstrates also includes the reference station's displacements, multipath and noise. Removing the common mode signal is not required when beam forming, as the common mode signal is naturally separated from other signals. Removing the common mode and beam forming the resulting absolute displacement time series, however, improves the signal-to-noise ratio for the seismic waves and facilitates automating the measurement of phase velocity and azimuth.

[3] Traditional GPS phase data is recorded at 30 s epochs and produces millimeter precision daily positions for tectonic and other applications [e.g., *Bock et al.*, 1986]. The continuously increasing number of geophysical observation types from these GPS data include: long-term secular plate motions [e.g., *Sella et al.*, 2002], and interseismic loading [*Kreemer et al.*, 2003], coseismic and postseismic fault movements [e.g., *Hudnut et al.*, 1994], details of active deformation associated with ongoing orogeny [e.g., *Brooks et al.*, 2003], aseismic slip or slow earthquakes from a number of tectonic environments [e.g., *Dragert et al.*, 2001], and nonsecular vertical loading from a variety of sources with periods of weeks to years [e.g., *vanDam et al.*, 1994a].

[4] As GPS technology and analysis techniques improved, it became possible to obtain displacements at each GPS measurement epoch with precision between 1 and 2 mm and a centimeter using kinematic processing [*vanDam et al.*, 1994b; *Hatanaka et al.*, 1994], instantaneous positioning [*Bock et al.*, 2000], differential processing [*Herring*, 2009a; *Larson et al.*, 2003], or precise point positioning (PPP) [*Kouba*, 2003]. PPP, which produces absolute position using a single GPS station, is currently less precise than the other methods, which use some form of differential or relative positioning between two or more stations.

[5] Relative displacement time series from the M_W 7.1, 1999, Hector Mine earthquake [*Nikolaidis et al.*, 2001],

[1]Center for Earthquake Research and Information, University of Memphis, Memphis, Tennessee, USA.

0148-0227/09/2009JB006288$09.00

produced using instantaneous positioning, clearly show displacements associated with the surface waves. *Nikolaidis et al.* [2001] used 30 s data and short baselines, 10–30 km, for sites between 50 and 200 km epicentral distance. Because the time series are aliased, as noted by *Nikolaidis et al.* [2001], they cannot provide meaningful information about either their time history or spectral content of the ground motion. In the epicentral region of moderate and larger earthquakes, Fourier components of ground motion with periods less than 1 min, the Nyquist limit for 30 s sampling, can have amplitudes of order cm or greater and faster data collection rates are needed to properly record such signals.

[6] Until recently, the paucity of HRGPS stations severely limited their use because the most precise processing, which produces relative positions, requires all the data used in the analysis to be collected at the same rate. The 2002, Denali earthquake was the first that was widely recorded at 1 Hz, and *Larson et al.* [2003] found displacements of kinematic stations in the epicentral area with respect to a distant reference station in Colorado. The reference station in Colorado was assumed to be stationary, which was true until the seismic surface waves arrived in Colorado where they were large enough to affect the GPS measurements. Before the surface waves arrived in Colorado, therefore, the relative displacement time series practically represented absolute displacements in Alaska since the station in Colorado was stationary. By the time the surface waves arrived in Colorado, seismic motion had died down in the epicentral area in Alaska, so the relative displacement time series then represented absolute displacements in Colorado. Absolute displacement surface waves from Denali were observed by HRGPS to distances of almost 4000 km by using long baselines and selecting the reference station such that it was not simultaneously affected by seismic waves.

[7] Using the instantaneous positioning method over short baselines in a small aperture network of four 1 Hz HRGPS stations in southern California, *Bock et al.* [2004] also observed surface waves from the Denali earthquake at an epicentral distance of 3900 km. Since the reference station in this case was also being simultaneously affected by the seismic waves the HRGPS time series represented relative displacements. Interpretation of relative displacement time series is problematic as these time series do not represent the motion due to the seismic waves at any single HRGPS station. *Bock et al.* [2004] compared sidereally filtered 1 Hz HRGPS displacement time series, both before and after spatial filtering, to absolute displacement seismograms from nearby broadband seismometers and found both agreed well at periods longer than 1 s, with better agreement for the spatially filtered data. We will show later that the spatially filtered time series in this case were actually absolute displacements.

[8] Since the Denali earthquake, HRGPS applications have also observed a wider range of large amplitude, weak motion, surface waves [*Ohta et al.*, 2006; *Takasu*, 2006] and captured near field coseismic offset and strong motion displacement time series that have been used independently or together with seismic data to invert for fault slip [*Larson et al.*, 2003; *Ji et al.*, 2004; *Miyazaki et al.*, 2004; *Kobayshi et al.*, 2006; *Emore et al.*, 2007]. Visually, HRGPS data from epicentral areas compares well with integrated strong motion data [*Ji et al.*, 2004; *Miyazaki et al.*, 2004; *Bock et al.*, 2004], but the question of sampling rates required to prevent temporal aliasing of very near field coseismic displacements using HRGPS data has not been properly addressed. Integration of strong motion records at epicentral distances of <5 km from M > 6 earthquakes, for example, shows that 1 Hz data there can be significantly aliased (Smalley, in revision). This is a pure signal processing consideration, as the signal being recorded, including any preconditioning antialias filtering that can be applied to limit the bandwidth, is the determining factor here, not the capability of the GPS receiver to track the GPS signal.

[9] The Great, 2004, M_w 9+, Sumatra-Andaman earthquake produced the first opportunity to apply HRGPS seismology on a global scale. This earthquake generated seismic waves of enormous amplitudes that clipped a large fraction of seismic recording systems globally. Sparse HRGPS data resolved strains of 6×10^{-6} and recorded displacements of 5–10 cm amplitude from surface waves at 2500–3000 km distance [*Ohta et al.*, 2006]. Absolute displacement time series were obtained for HRGPS stations on Diego Garcia and Jakarta at 2000 to 2500 km epicentral distance using differential processing and reference HRGPS stations in Kenya and Japan at over 6000 km epicentral distance [*Ohta et al.*, 2006]. The surface waves took ~10 min to arrive at the kinematic stations and ~25 min to arrive at the reference stations. This time difference left an ~15 min window in which absolute displacements could be found using differential processing. The distance between the stations being affected by the seismic waves and the reference station, which is restricted to being outside the area affected by the seismic waves, is limited by the differential processing requirement that all stations see a set of common satellites. This condition limits the distance between the reference and nonreference stations, which restricts the time window available to obtain absolute displacements. For an earthquake as large as the Sumatra-Andaman event, which affected the whole earth, the conditions on the reference station make it difficult to obtain absolute displacement time series during the time range over which surface waves pass by a given location.

[10] Using PPP, which produces absolute displacements for a single station, *Takasu* [2006] reported detection of absolute displacements associated with surface waves from the earthquake to a distance of 13,000 km, which is less than the distance at which they can be both observed and analyzed with relative positioning. In addition to the dynamic, transient seismic waves, the earthquake also produced a static coseismic displacement field that was measured using GPS. *Ohta et al.* [2006] were unable to observe any such displacement from integration of the HRGPS displacement data, but *Kreemer et al.* [2006], using standard daily processing, found ~4 mm of coseismic offset for the GPS station on Diego Garcia and coseismic offsets that are at least 1mm in magnitude globally.

2. Sumatra-Andaman Seismic Waves in Central North America

[11] The back azimuth to the Sumatra-Andaman earthquake from central North America (CNA) is ~N, which results in the seismic waves being naturally polarized in the

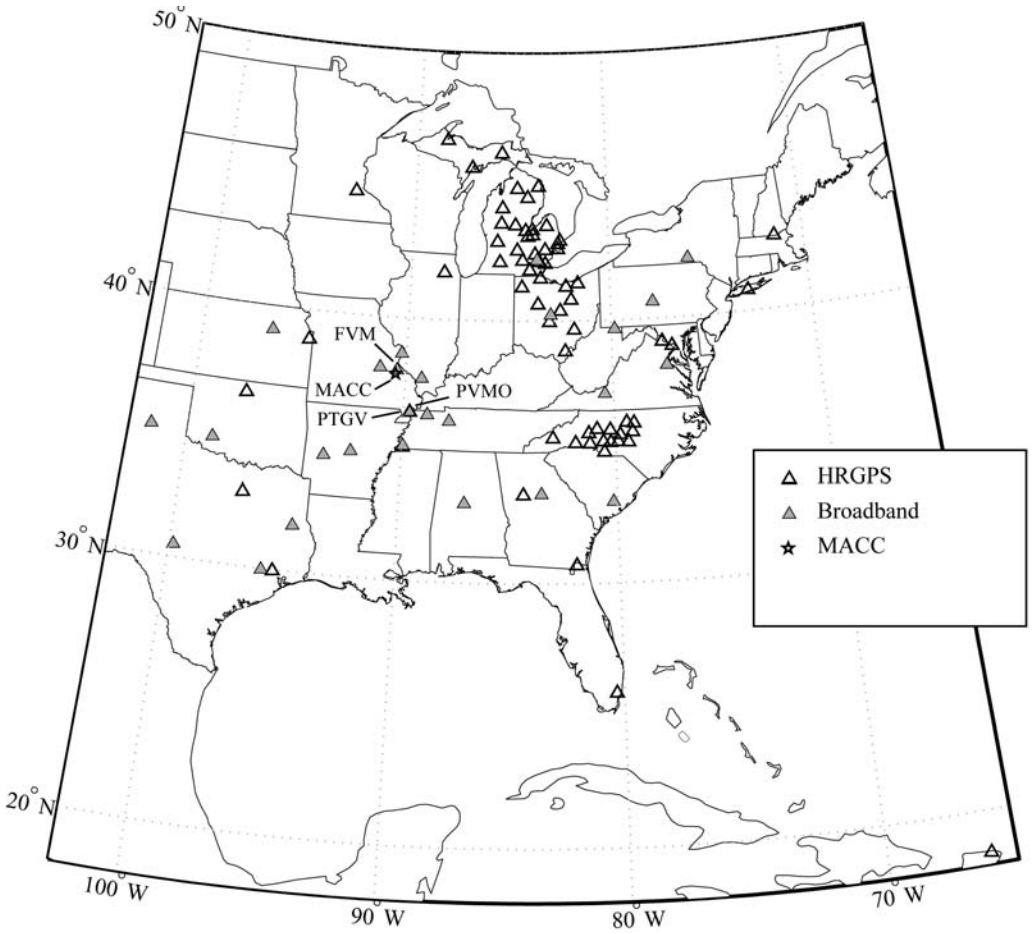

Figure 1. Map of HRGPS (open triangles) and broadband seismometers (gray triangles) used in this analysis (except one HRGPS station far to the north in Canada, CHUR, and one far to the south in Bogotá, BOGT). HRGPS stations PTGV (bold gray triangle) and MACC (star) are approximately colocated with broadband seismometers PVMO and FCM, respectively (all labeled). PTGV and MACC are on stable geodetic monuments designed for tectonic studies. The dense groups of HRGPS stations are networks operated by the states of Michigan, Ohio and North Carolina, while the more disperse stations are mostly from the U.S. Continuously Operating Reference Stations (CORS) and the Federal Aviation Administration (FAA) networks. These networks were built to support surveying activity or air navigation, and most of the antenna monuments are less stable than those installed for scientific studies. During the several hour period of interest of this study, however, these monuments are sufficiently stable.

geographic coordinate system used by both GPS and seismology. The ∼N-S strike of the fault and the ∼west directed thrusting also place CNA in the maximum and minima, respectively, of the Love and Rayleigh wave radiation patterns. Love waves, with periods >60 s and peak-to-peak displacement amplitudes >4 cm, were well recorded by broadband seismometers in CNA at epicentral distances of over 14,000 km. Displacements this large should be easily measurable with GPS. At the time of the Sumatra-Andaman earthquake, two 1 Hz HRGPS stations (PTGV and MACC) of the GPS Array for Mid-America (GAMA) were operating in the New Madrid seismic zone of central North America (Figure 1). We used the TRACK kinematic GPS processing module [*Chen*, 1998; *Herring*, 2009b, 2009c] of the GAMIT/GLOBK package [*King and Bock*, 2000; *Herring*, 2009a] to produce kinematic HRGPS relative displacement time series in which Love waves are clearly observed (Figure 2, middle).

[12] The two GAMA HRGPS stations are approximately collocated with two broadband seismic stations, PVMO and FVM, respectively, of the Cooperative New Madrid Seismic Network (Figure 1). HRGPS station PTGV is ∼5 m from the broadband seismometer PVMO, while HRGPS station MACC is ∼15 km along raypath distance from the broadband seismometer FVM. The MACC to FVM spacing is much less than a seismic wavelength for waves with a period greater than about 20 s, and we will consider them collocated. Since both HRGPS stations were simultaneously affected by the surface waves, the kinematic GPS analysis produces a single time series of the relative position between the two stations rather than a time series of absolute positions for each. To compare the HRGPS relative displacement time series to the broadband seismometer data, we calculated a relative displacement seismogram using data from the two seismic stations. As the broadband seismometers record velocity, we removed the instrument

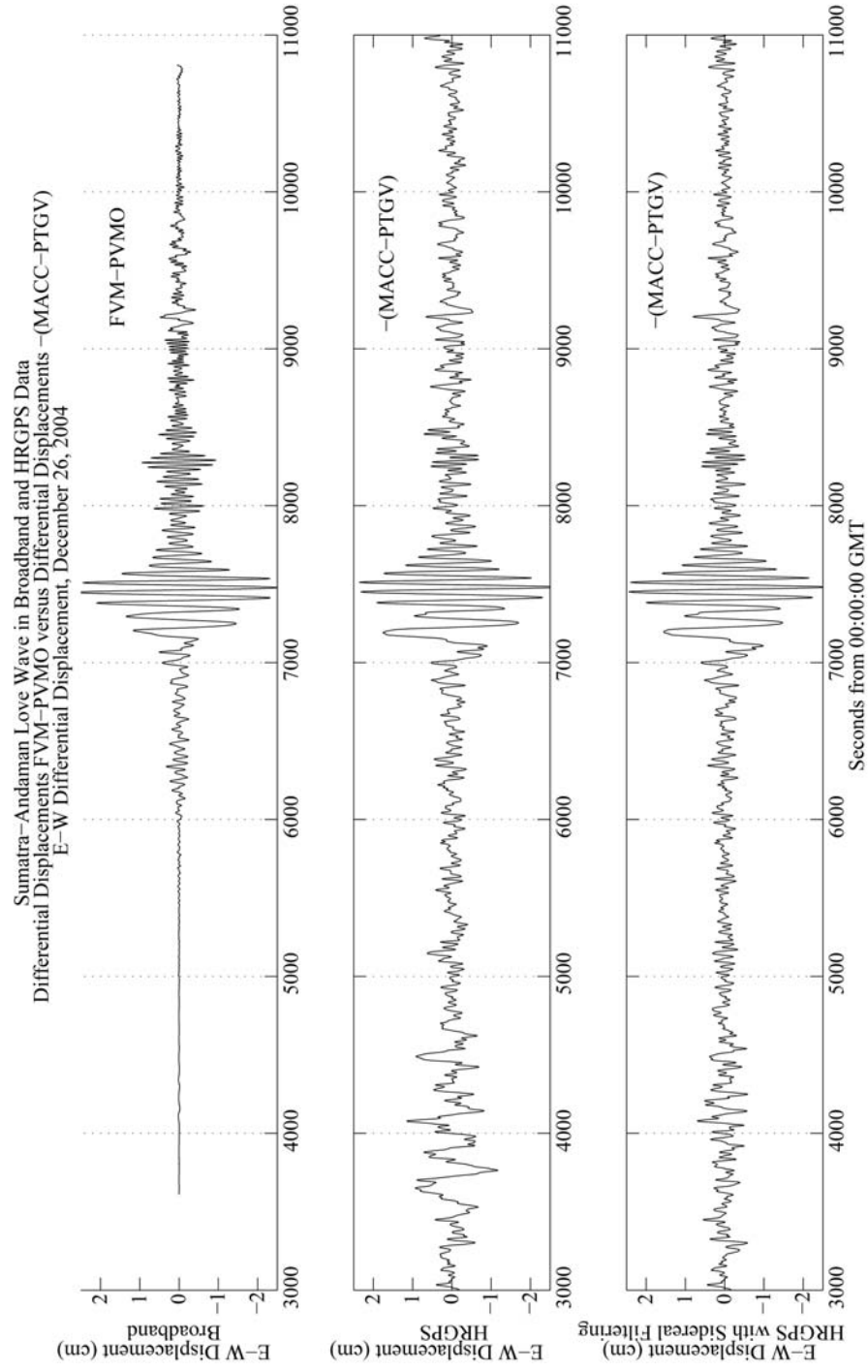

Figure 2. Comparison of relative displacement seismograms from a pair of approximately collocated HRGPS (PTGV and MACC) and broadband seismometers (PVMO and FVM). (See Figure 1 for station locations.) (top) Trace is relative displacement for the broadband seismometer data. (middle) Trace is HRGPS relative displacement time series before modified sidereal filtering. (bottom) Trace shows the same data after applying modified sidereal filtering. The difference between the seismic and HRGPS time series at the beginning of the dispersed wave train is due to the flat response of HRGPS, and, therefore, continued sensitivity at longer periods, in comparison to the seismometer response, which rolls off at periods longer than 300 s.

response, integrated velocity to displacement, and differenced the two absolute displacement seismograms to produce a relative displacement seismogram (Figure 2, top). We did not adjust for the difference in travel time due to the difference in path length between MACC and FVM in the calculation of the differential seismogram. The travel time difference is not a constant, it varies from 3 to 4 s with frequency due to dispersion of the surface waves. A large packet of Love waves is clearly visible in both the broadband and HRGPS relative position time series (Figure 2, top and middle). The large amplitude, long period "signal" at the beginning of the relative displacement HRGPS time series (Figure 2, middle) is due to GPS multipath. Multipath is a generic term for the reception of multiple, interfering versions of the same signal. In the case of GPS, the most significant source of multipath is the reflection of the GPS signal from objects in the vicinity of the antenna. GPS multipath can be attenuated, but not completely removed, by sidereal [*Bock et al.*, 2000] or modified sidereal filtering [*Larson et al.*, 2003; *Choi et al.*, 2004] (Figure 2, bottom). For a fixed GPS station, the receiver and the geometry of local reflectors of the GPS signal are assumed to be fixed in time, but the transmitter geometry varies in time with satellite position. As GPS orbits approximately repeat each sidereal day, at any given sidereal time, the GPS multipath environment, consisting of the instantaneous geometry of the satellites, receiver, and reflectors, should be the same and produce the same GPS multipath effect. *Genrich and Bock* [1992] used this observation to propose a GPS multipath mitigation technique, sidereal filtering, in which apparent displacements due to GPS multipath are estimated using data from nearby sidereal days otherwise free of displacements, i.e., no seismic waves [*Bock et al.*, 2000]. *Choi et al.* [2004] further developed the method, renamed modified sidereal filtering, by using cross correlation of the 1 Hz HRGPS displacement time series during aseismic periods to provide a better estimate of the sidereal time shift. Sidereal and modified sidereal filtering are both implemented in the time domain and significantly reduce GPS multipath, but do not remove it completely.

[13] Seismic waves can also be affected by multipath, and we will use the adjectives "GPS" or "seismic" to distinguish between the two types. Seismic multipath is part of the seismic signal in the earth and often produces quantifiable features in the array processing analysis that can be used to estimate errors in the determination of azimuth and velocity. Seismic multipath affects both the seismometer and HRGPS derived displacement time series. The packet of waves that arrives at about 9000 s (Figure 2) is the R2 Love wave that comes the long way around the earth (this is a simple, and easily identified, form of seismic multipath).

[14] Based on the clear signal observed in the HRGPS seismograms from the GAMA stations, we obtained additional data from the Sumatra-Andaman earthquake at over 130 1 Hz HRGPS stations, of which over 90 provided usable data, and 28 broadband seismometers in CNA (Figure 1) for further analysis and application of HRGPS seismology. Most of these HRGPS stations were installed and are operated by the Federal or State governments to support surveying, state or national geodetic reference frames, and navigation. As such, most of the antennas in these networks are not mounted on the types of highly stable monuments typically used for tectonic GPS studies. The monuments, however, are more than sufficiently stable for HRGPS seismology during the few hour period during which the seismic waves passed by. For the case of weak motion, we assumed that the instrument response, or transfer function, of the GPS antenna mounting, or monument, is 1.

[15] Relative displacement time series (Figures 3a, 3b, 4a and 4b) were obtained with TRACK [*Herring*, 2009b, 2009c, also personal communication, XXXX] using the station PTGV (Figure 1) as the reference station and IGS orbits. In order to improve the beam steering results, we applied a Hanning window, $HW = 1 + \cos(\pi(-1 + 2*t/5100))$, $0 \leq t \leq 5100$, to the time series shown in Figures 3a and 3b and used in the beam steering. The majority of baselines to the reference stations were in the range of 500 to 1200 km (Figure 5). While TRACK can solve for a small number of kinematic sites in a network solution, we found the processing to be more stable if we processed each kinematic station individually. TRACK uses double differences to estimate the positions, and the quality of the solution depends on the success of fixing the GPS phase ambiguities to integer values. (Geodetic precision GPS processing uses measurements of the phase of the GPS signal.) As in the analysis of seismic surface waves, phase measurements are ambiguous with respect to the number of whole cycles between two measurements. Just as one needs to estimate the number of whole (integer) cycles between the hypocenter and seismic stations to calculate the spectral phase of the signal at the source [see, e.g., *Brune et al.*, 1960; *Nafe and Brune*, 1960], one needs to estimate the number of whole cycles between the GPS receivers and the GPS satellites at the time of the measurement to obtain the range or distance. The undermined number of full cycles are known as "ambiguities," or "integer ambiguities," in GPS processing. The GPS data were initially processed to tune TRACK's command file and processing options. The final time series for each station was produced in a run of TRACK using these tuned options (T. A. Herring, personal communication, XXXX). Eliminating sites with large jumps, small maximum amplitudes, or obvious data or processing problems reduces the number of stations for further processing to 92. The selected time series were windowed to include the 5100 s period during which the surface waves were crossing the whole network and band pass filtered between 1100 and 12.5 s period.

3. Data Analysis

[16] At regional to teleseismic distances the seismic wavefield is sufficiently coherent that array processing beam forming can be applied to dense samplings of the wavefield. While array processing is common and well understood in seismology [e.g., *Burr*, 1955; *Burg*, 1964; *Green et al.*, 1965, *Frosch and Green*, 1966; *Whiteway*, 1966; *Gangi and Disher*, 1968; *Capon*, 1969], it is worthwhile to present a short review here to point out some differences in its application to HRGPS time series "seismograms." Array processing analyzes multiple samplings of a wavefield in both time, using seismograms, and space, using simultaneous

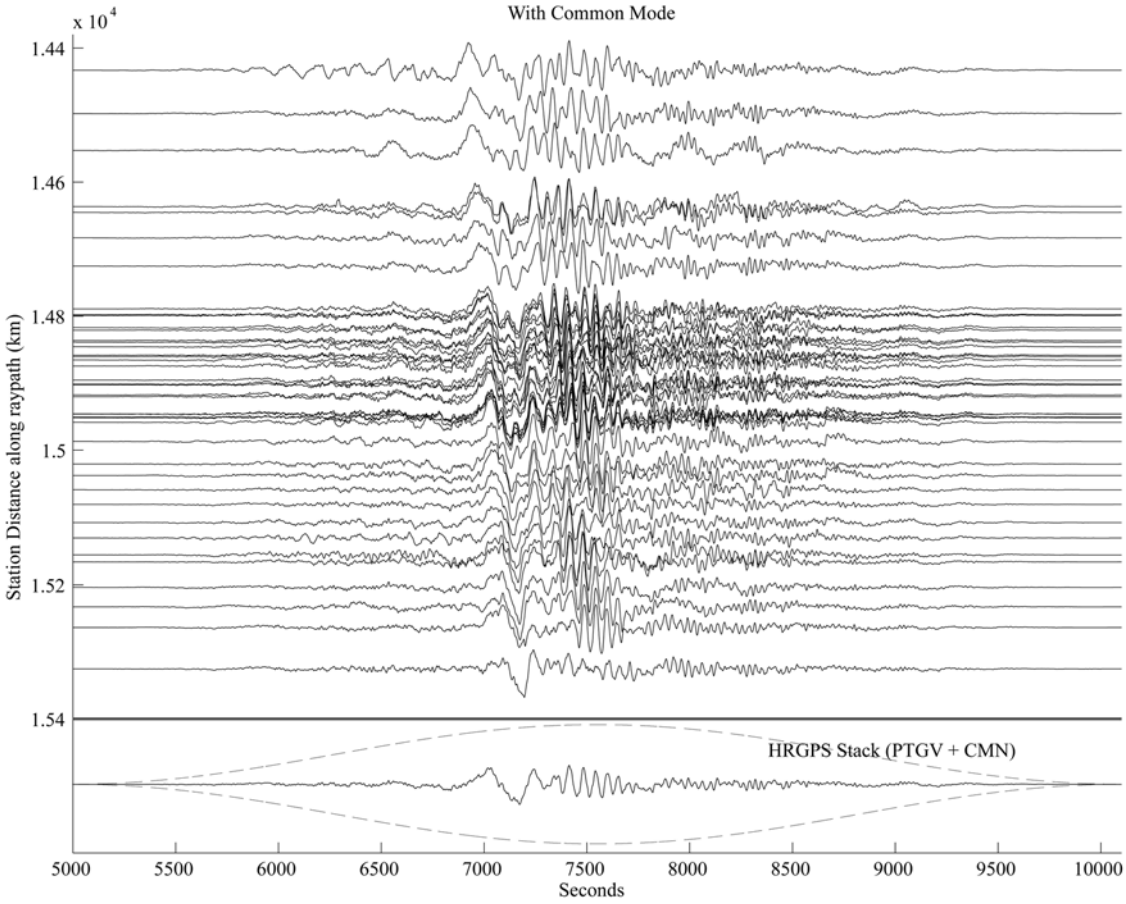

Figure 3a. Record section of HRGPS relative displacement time series, band-pass filtered from 0.01 to 0.02 Hz, through the Michigan and Ohio section of the array. Large amplitude Love surface waves are clearly observed. The individual trace at the bottom shows the absolute displacements of the reference site estimated using the $\vec{k} = 0$ beam of the array as discussed in the text. A Hanning window (shown by the dashed envelope about the bottom trace) has also been applied to all the data. This is why the traces have much lower amplitudes at the beginning and end.

sampling from seismograms at different locations. To illustrate the basics of array processing, consider the D'Alembert traveling wave solution to the wave equation, $f(\vec{k} \bullet \vec{x} \pm vt)$. This solution describes a wave that is a function of the argument $A = (\vec{k} \bullet \vec{x} \pm vt)$, and not x and t individually, traveling with constant velocity, v, in the direction given by the wave number $\vec{k}$. The shape of the wave in space, a snapshot, is constant and given by $f(A)$. The position of the wave at any time, t, is determined by the relationship between x and t in the argument. We can, therefore, take snapshots of the wave at different times and line them up by shifting each appropriately, where the shift is determined by the direction, $\vec{k}$, and speed, v, of the wave. Once the snapshots are lined up, we can add them together to obtain an estimate of $f(A)$ with an improved signal-to-noise ratio. This process of shifting and adding is known as beam forming, and each shift represents a beam that is sensitive to a specific direction and velocity. Since f is not a function of either x or t individually, position and time shifts are interchangeable, but related in the snapshot and seismogram views of the data. Each of the beams is a stack, and stacks calculated with shifts are often called slant stacks. In 2-D the beam form is given by

$$z(t, \delta t_{l,m,n}) = \frac{1}{N}\sum_{n=1}^{N} r_n(x_n, y_n, t + \delta t_{l,m,n});\ \delta t_{l,m,n} = -\frac{\vec{k}(l,m) \bullet \vec{x}_n}{\omega} = \vec{s}(l,m) \bullet \vec{x}_n.$$

The time shifts $\delta t_{l,m,n}$ are determined by the slowness, $\vec{s}(l, m)$, of the beam being formed. Slowness is the inverse of velocity,

$$\vec{s}(l,m) = \frac{1}{|\vec{v}|}\frac{\vec{v}}{|\vec{v}|} = \frac{\vec{k}(l,m)}{\omega},$$

and is parallel to $\vec{k}$ and $\vec{v}$. The l, m terms are associated with the x, y components, respectively, of the wave number or slowness vectors.

[17] For a beam whose slowness matches that of a wave crossing the array, the seismograms interfere constructively to produce a large signal with reduced noise, while in all other beams the seismograms interfere destructively resulting in cancellation. While beam forming is typically

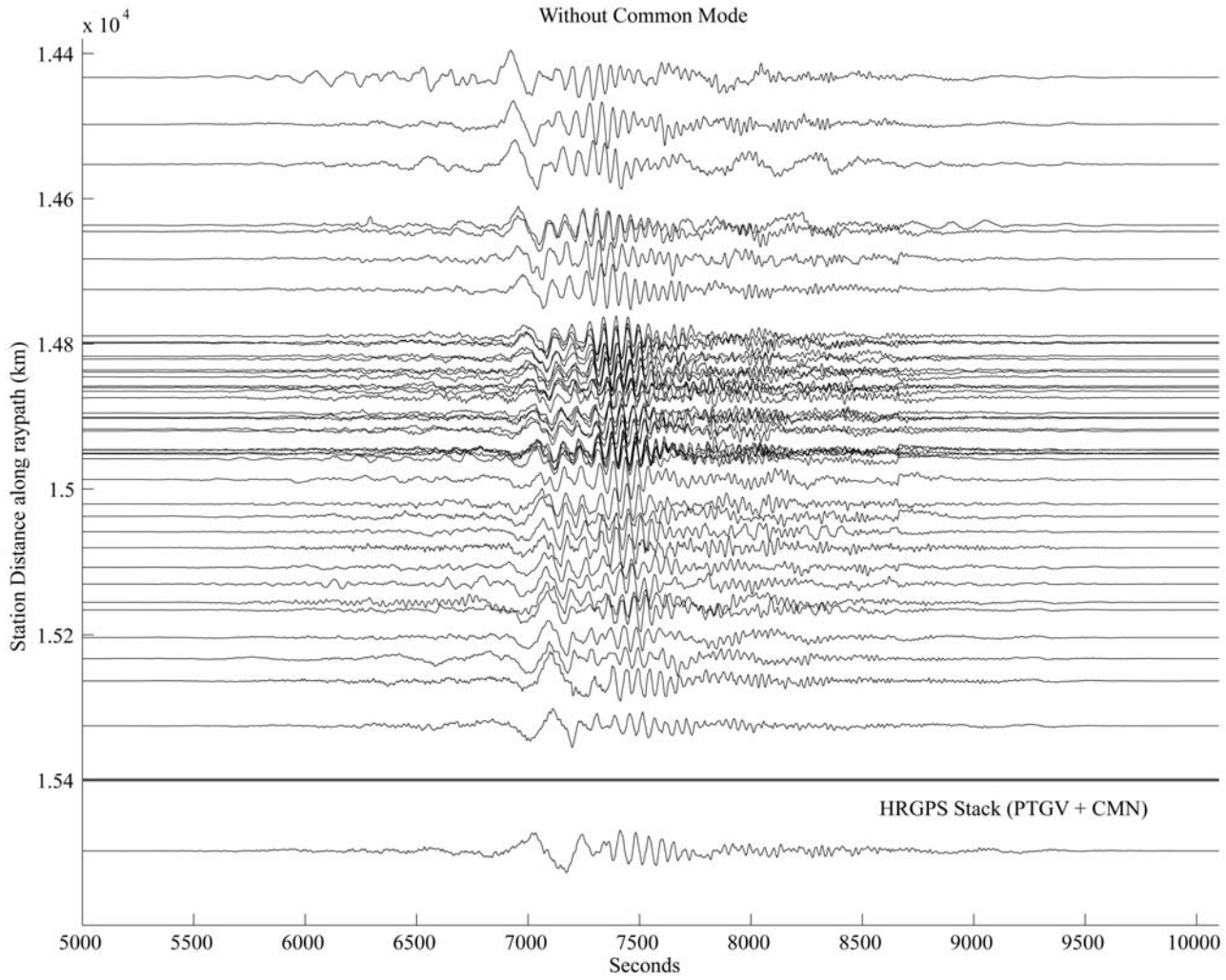

Figure 3b. Same as Figure 3a but for absolute displacement time series formed by subtracting the absolute displacement of the reference site.

presented in the real distance and time domains, the computations are typically carried out in the frequency domain. Fourier transforming the time domain beam form, we obtain

$$Z\left(\vec{k}(l,m),\omega\right) = \frac{1}{N}\sum_{n=1}^{N} R_n(x_n,y_n,\omega)e^{-i\vec{k}(l,m)\bullet\vec{x}_n};$$

$$R_n(x_n,y_n,\omega) = \int_{-\infty}^{\infty} r_n(x_n,y_n,t)e^{-i\omega t}dt.$$

Working in the frequency domain facilitates analysis of dispersed waves, such as seismic surface waves, where the Fourier components at different frequencies, ω, travel at different velocities, $v(\omega)$. Dispersed waves do not correspond to D'Alembert's solution as the variation of velocity with frequency causes the shape of the wave to change as the wave propagates. The wavefields in the snapshots at different times are now different, and one cannot globally line up the wavefield in two snapshots. By performing the beam forming on band pass filtered versions of the seismograms, we can remove this variation and analyze wave properties such as apparent velocity as a function of frequency.

[18] All arrays have a response based solely on their geometry. This response defines their resolution, or ability to separate two different wave numbers or slownesses, and gain, which determines the minimum signal/noise ratio to observe a signal. The response of an array of regularly spaced sensors is shown in Figure 6a. In general, arrays with nonuniform or random spacing of the sensors have lower gain than regularly spaced arrays (Figure 6b, which shows the response of the array in Figure 1). In the regularly spaced array for example, the first side lobe to the north is about 12 dB down, while in the nonuniform array it is about 7 dB down. The response of nonuniform or irregular arrays can be improved by weighting [*Holm et al.*, 1997], although this changes the response from linear to nonlinear. If the noise is uncorrelated, beam forming also increases the signal/noise ratio by $\sqrt{N}$. The response of both regularly and irregularly spaced arrays can be improved by nonlinear techniques such as maximum-likelihood processing [*Capon et al.*, 1967], or *N*th root stacking [*Kanasewich et al.*, 1973]. While such techniques are useful when the signal-to-noise ratio is very low, they distort the wave form, so they cannot be used for the generalized spatial filter.

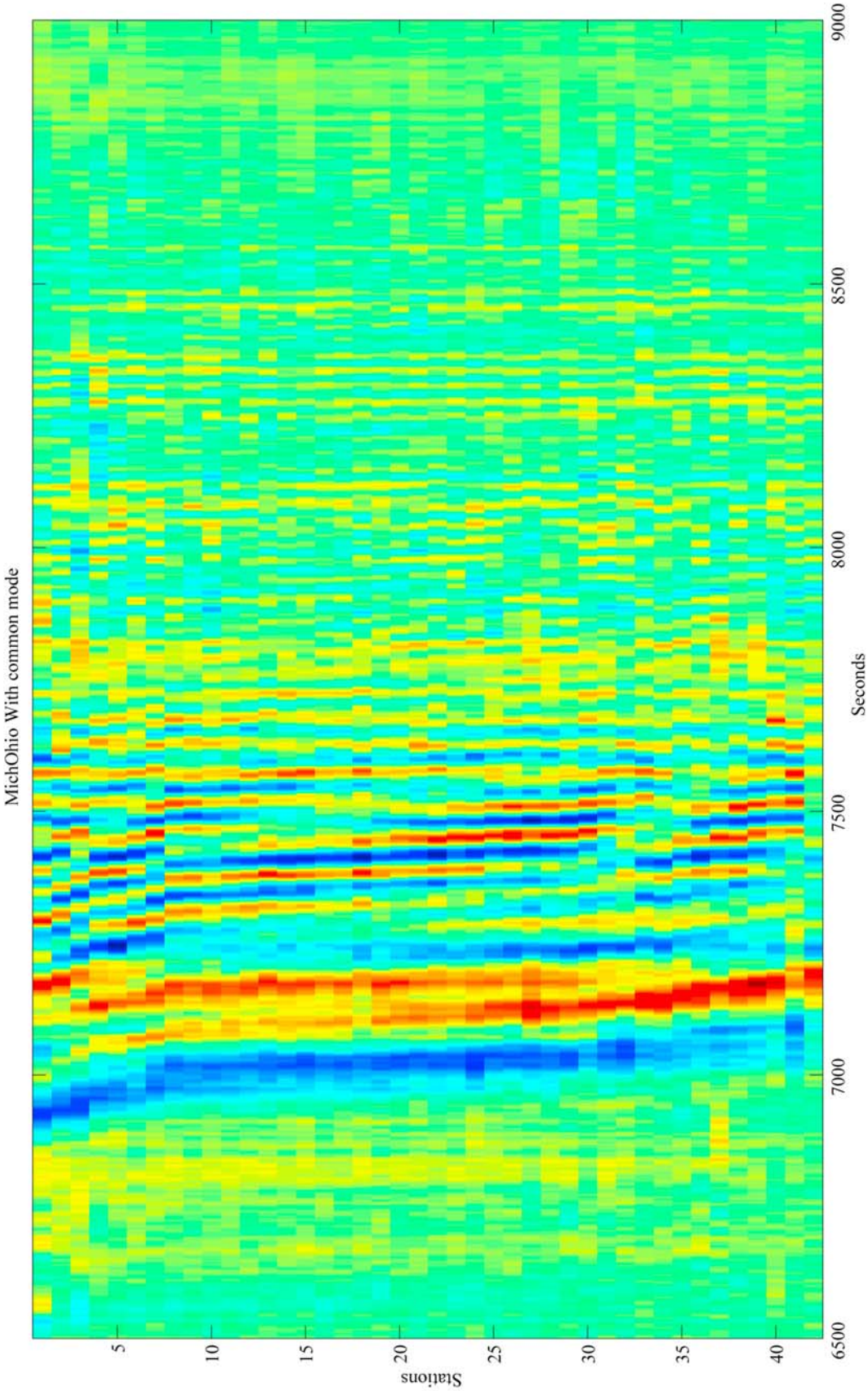

Figure 4a. View of the seismic portion of the HRGPS relative displacements shown in Figure 3a as a surface plot which illustrates the coherence of the surface waves and the data quality. This is not a record section; the vertical axis is station number ordered by distance. Note the two distinct low frequency red crests on the top left, between 2000 and 2400 s, which merge into one crest as the epicentral distance increases (downward). The crest that moves out, or tilts, to the right as distance increases is that of a single seismic surface wave crossing the array at surface wave velocity. The crest that is vertical is the same crest of the surface wave but at the reference station, and it is found simultaneously at all the kinematic stations as a common mode with infinite velocity. For the higher frequency crests farther to the right, one observes vertical sections that shift with respect to one another as the distance changes, but it is not obvious that this field is composed of two waves, one moving across the array at a finite velocity and one at an infinite velocity.

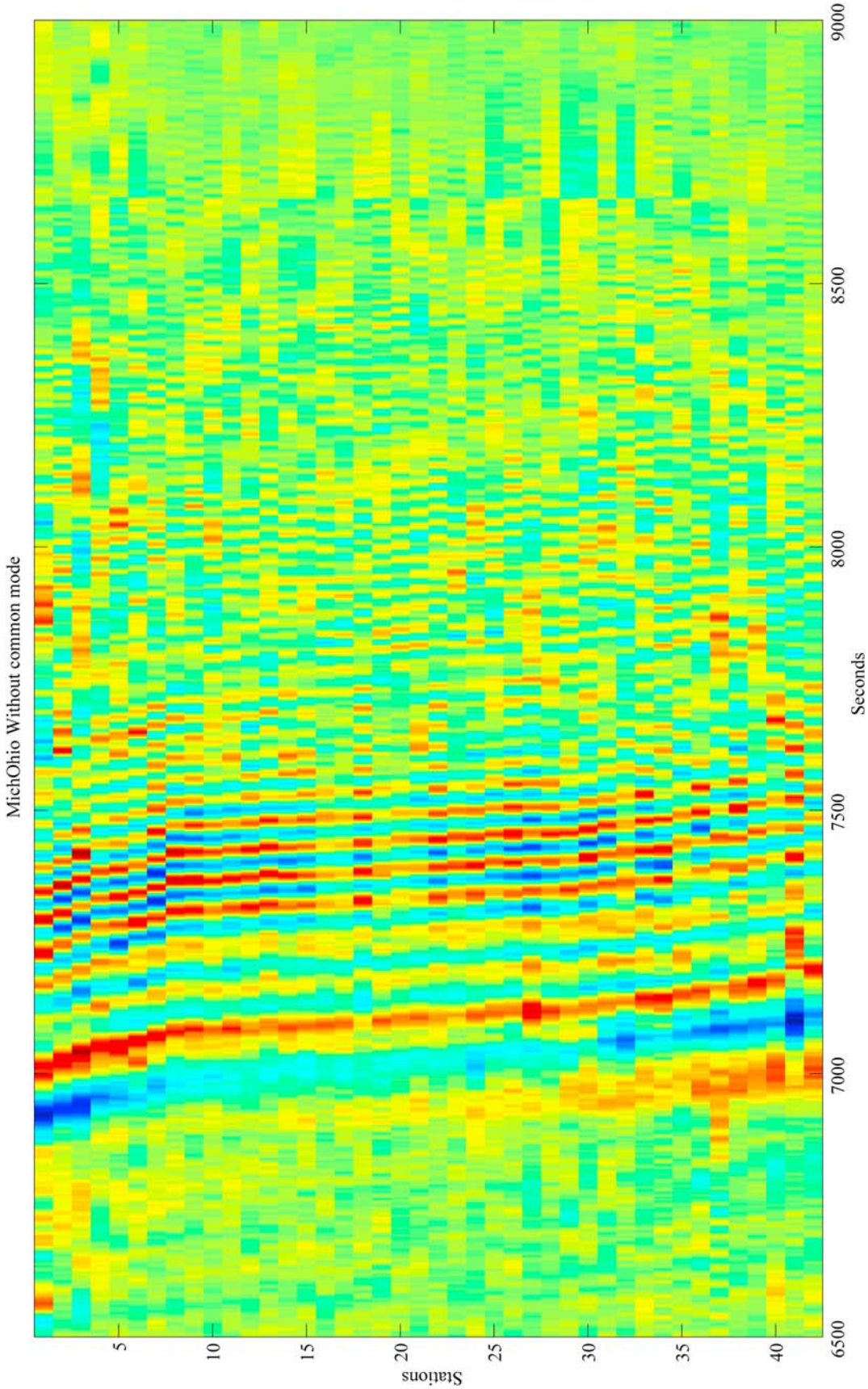

Figure 4b. Presentation as in Figure 4a for the seismic portion of the HRGPS absolute displacements shown in Figure 3b. We now see a clear series of crests, starting at low frequency on the left and becoming higher in frequency on the right due to dispersion, that move out and can be followed continuously as the waves cross the array.

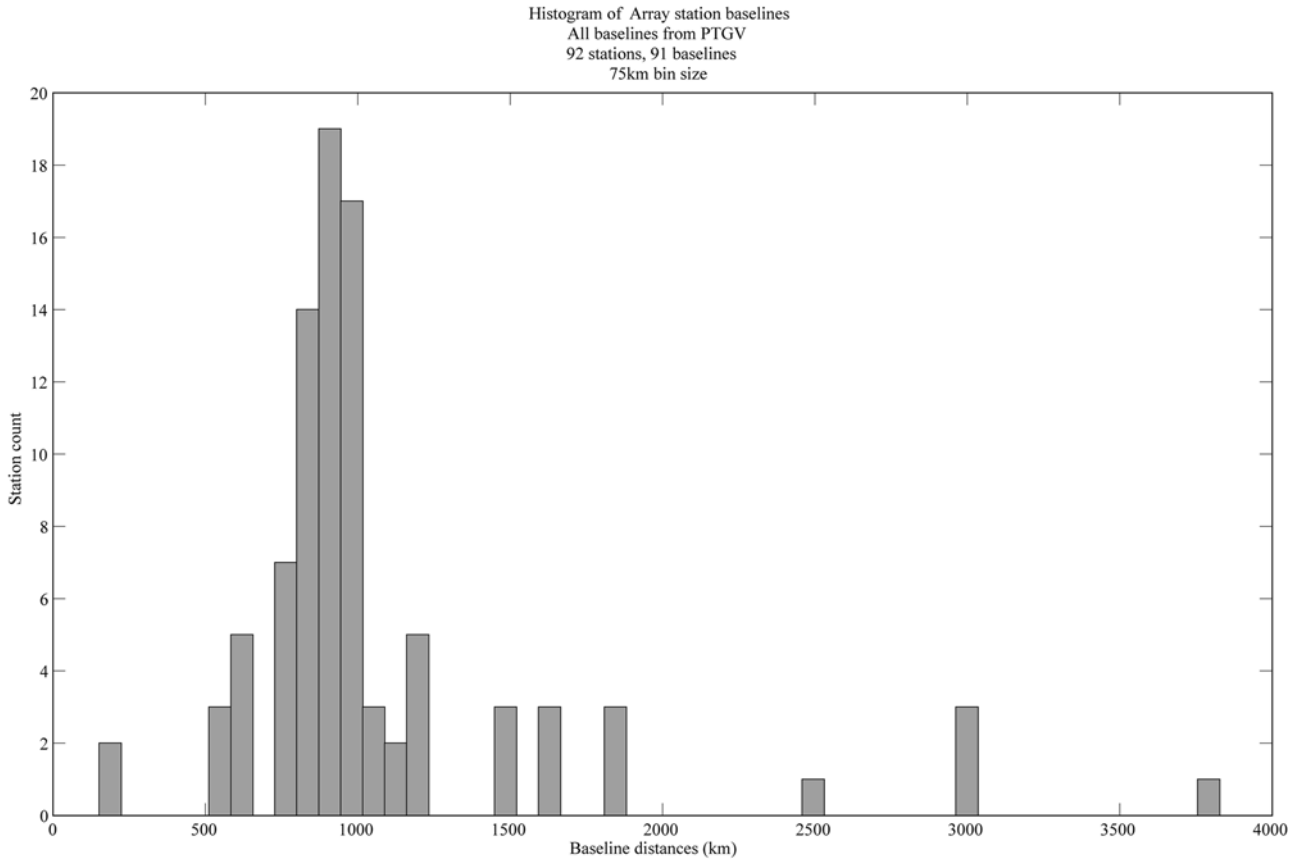

Figure 5. Histogram showing baseline lengths from the reference station, PTGV.

[19] In order to analyze the spatial recording of the wave in the frequency domain, we must have two or more samples per wavelength, the Nyquist condition in space rather than time, to prevent spatial aliasing. This condition defines the short wavelength limit of the array. If the frequency domain representation of the seismic waves has wavelengths shorter than this value with sufficient amplitude to be measurable by HRGPS, the data will be spatially aliased, and array processing may not provide useful information. Unfortunately, it is not possible to implement a spatial antialias filter, so one has to have an independent estimation of the signal to assure that aliasing is not occurring. The problem of spatial aliasing is reduced in the nonuniform or randomly spaced array. This can be seen by comparing the sampling of two arrays, one uniform and one nonuniform, where the spacing of the uniform array is equal to the spacing of the nonuniform array (Figures 6a and 6b). In a random array, the spacing between half the stations will be less than the average. Although for nonuniform or random arrays, there is no simple rule for the minimum wavelength, as is the case for a regular array. The smaller spacing in the nonuniform or random array allows nonaliased recording to shorter wavelengths than that of the regular array. Ordering the stations by epicentral distance and examining the along raypath spacing between adjacent stations, about half the separations are less than 10 km. This indicates that spatial aliasing will not occur for wavelengths greater than about 20 km, which corresponds to periods longer than about 10 s.

[20] The array also has a limitation on the longest resolvable wavelength, which is on the order of the aperture of the array. For waves with wavelengths larger than the aperture of the array, to first order the array sees such waves as a common mode effect. If we consider the central, dense,

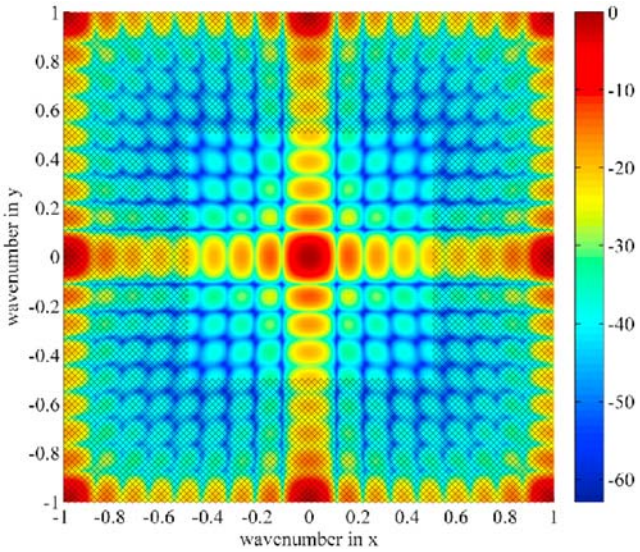

Figure 6a. Array response for a uniform nine by nine array. The hachured area outside the central portion from ±0.5 in both x and y represents the region in which the uniform array records aliased data.

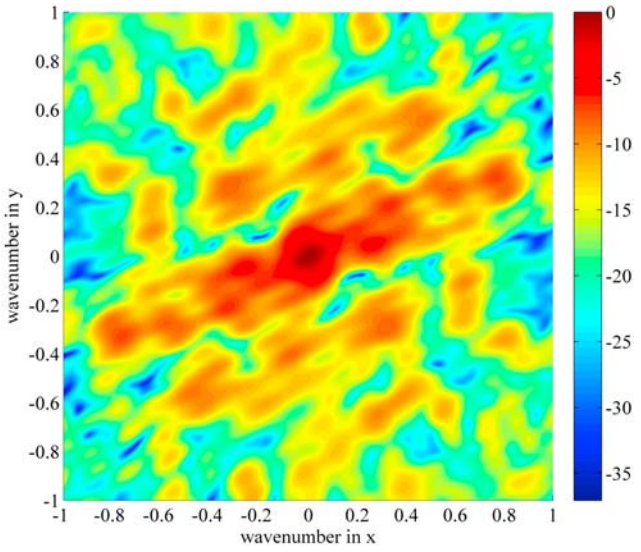

Figure 6b. Array response for nonuniform array of GPS stations used in this study. This array has a central response similar to that of the uniform array, but the side lobes are higher. One can also see that the nonuniform array is strongly asymmetric. It has better resolution in NNW-SSE direction than in the ENE-WSW direction. This is due to the overall denser spacing along the NNW-SSE direction. The array response can be tuned for symmetry or "spot" size by selecting a subset of the available stations. The direction of highest resolution is close to optimal for the direction of the seismic waves. Aliasing does not occur in the range of k values shown for the nonuniform or random array.

portion of the array shown in Figure 1, removing the northernmost and two southernmost stations, the aperture is approximately 1000–1500 km, which at a velocity of 5 km/sec corresponds to waves of 200–300 s period. For waves in the proper range of wavelengths, beam forming can determine the azimuth and phase velocity of waves crossing the array directly. Beam forming can also used as a basis for frequency-wave number filtering ($f - \vec{k}$ filtering) which filters both the temporal and spatial components of the data. A simple model, which we present below, suggests that $f - \vec{k}$ filtering of HRGPS data can be used to improve GPS multipath mitigation.

[21] For a single plane wave crossing the array, beam forming shifts the array response from the origin to a location in (k_x, k_y) space centered on the wave's $\vec{k}$ vector. Using superposition, if several plane waves, with the same frequency but different directions, simultaneously cross the array they will each contribute a scaled, shifted copies of the array response to the beam form, producing multiple peaks. We will show that this ability to differentiate waves with the same temporal frequency content based on their spatial frequency characteristics, such as apparent velocity or slowness and azimuth, (1) provides a way to estimate the combination of common mode noise and the reference station's absolute displacement, noise and GPS multipath and (2) inherently reduces the effect of GPS multipath in array processing. The reduction in GPS multipath comes from the observation that GPS multipath is incoherent and, therefore, has little effect on beam forming measurements of the coherent seismic waves. Seismic multipath, on the other hand is typically a coherent signal, which is caused by a number of seismic waves crossing the array at the same time from slightly different directions. Seismic multipath has the effect of widening the peak azimuthally; causing error in the estimated azimuth.

4. Array Processing Results

[22] A beam form of band-passed, HRGPS differential displacements is shown in Figures 7a and 7b. Notice that there are two significant peaks of approximately the same amplitude. This is interpreted as representing two plane waves. One, in the top center, crosses the array at a finite apparent velocity appropriate for the phase velocity of surface waves. The second, whose amplitude is slightly larger, is at the origin and crosses the array at an infinite apparent velocity. This demonstrates that the kinematic HRGPS differential displacement time series for each non-reference kinematic station, T_n, can be modeled as being composed of two waves,

$$T_n = A_n + A_\infty,$$

where A_n is the measured absolute displacement at the kinematic station and A_∞, is a common simultaneous, infinite apparent velocity, signal that appears across the whole array.

[23] In Figure 8 the $\vec{k} = 0$ beam, or stack, responsible for the central peak is shown together with the absolute displacements obtained from the collocated broadband seismometer PVMO. The agreement between the two time

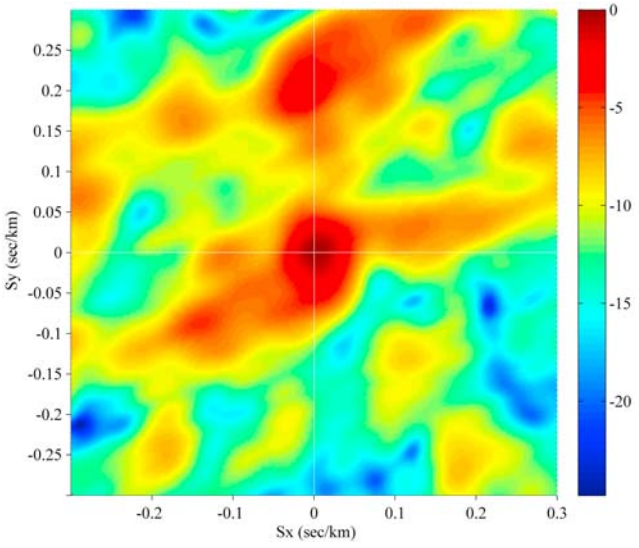

Figure 7a. Color contour plot of the beam form for band-passed (0.006–0.008 Hz), differential displacements showing double peak (two copies of the array "spot" from Figure 6b), one at the center from the reference station and common mode noise and a second one for the Love wave crossing the array with a slowness of 0.22 s/km, or 4.5 km/sec phase velocity, and back azimuth of ~N, determined by the peak position. The axis are plotted in terms of slowness, $s = 1/\nu$, rather than wave number, $k = s\omega$, to facilitate the comparison of slowness as a function of frequency.

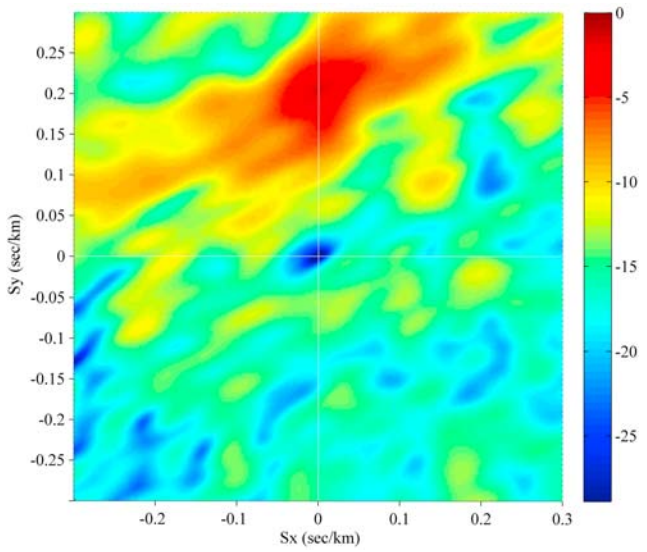

Figure 7b. Same as Figure 7a using absolute displacements, calculated as discussed in the text, now has a single peak with the same slowness but a slightly different (rotated <5° north) back azimuth.

series shows that the $\vec{k} = 0$ beam is a good estimation for the absolute displacements there. The $\vec{k} = 0$ beam includes all signals that appear simultaneously at each element of the array including common mode noise from the GPS processing and the GPS multipath and noise from the HRGPS station PTGV. We can, therefore, write

$$A_{\infty} = A_{cmn} - A_{ref} \text{ and } T_n = A_n + \left(A_{cmn} - A_{ref}\right),$$

where A_{ref} is the combined absolute motion, GPS multipath and noise of the reference station and A_{cmn} is the common mode noise. Since the common mode noise and reference station contribution have the same spatiotemporal characteristics across the array, they cannot be separated or obtained individually using array processing.

[24] Given N HRGPS stations, we therefore have $N - 1$ copies of the absolute displacements, GPS multipath, and noise of the reference station plus the common mode noise linearly combined with the absolute displacement, GPS multipath, and local noise of each kinematic station. When we form the $\vec{k} = 0$ beam, the randomly located kinematic stations randomly sample the wavefield and their movements should be incoherent at any given time (snapshot) and destructively interfere in the stack in which uncorrelated noise is reduced by a factor of $\sqrt{N-1}$. (The nonuniform array in Figure 1 is not truly random, but the approximation is valid.) We investigated using a weighting scheme in the beam forming based on station density as a function of the wavelength to down-weight coherent signals between nearby stations but found little improvement and, therefore, used an unweighted stack. The success of estimating the displacements of the fixed site will depend on both the size of the array (larger is better) and how close to random the irregular spacing of the GPS network actually is.

[25] An advantage of estimating the reference station's displacements from the HRGPS data itself, rather than using a colocated broadband seismometer, is that the HRGPS data also estimate, and, therefore, remove from the nonreference station's time series, the GPS network's common mode noise and the reference station's noise and GPS multipath. Another important advantage of estimating the reference station's absolute displacements, whether by stacking or using colocated broadband seismometer data, is that the reference station no longer has to be stationary by being outside the region being affected by seismic waves. This removes the requirement for extremely long baselines, the limitations on the length of the absolute displacement seismic time series that can be produced and the need for a set of multiple reference stations that roll away from the epicenter with time. The ability to use shorter baselines also significantly improves relative displacement processing compared to longer baselines as the satellite geometry is stronger and ambiguity resolution more robust.

[26] After removing the absolute displacements using the $\vec{k} = 0$ beam or stack (Figures 3b and 4b), beam forming of the new time series has a single, clear peak at the azimuth and apparent slowness, or wave number, of the seismic waves (Figure 7b). We now have only one wave crossing the array, and the peak at the center has been completely removed. Note that without returning to the time domain, the result of the beam forming is immediately providing geophysically useful information. Repeating the analysis for a range of frequencies, for both HRGPS and seismic data, we determined phase velocity versus frequency (Figure 9). The seismic and HRGPS results agree well, both between themselves and also with respect to observed and theoretical Love wave dispersion curves between 20 and 300 s periods, after which the seismometer response falls off for longer periods and the seismic results become unreliable. The HRGPS data continues to have coherent energy at periods from 300 to 500 s, but the wavelengths are becoming too long with respect to the array aperture, and the results of beam forming become unstable. This can be addressed with a larger aperture array or other types of processing. At the longest periods, long period multipath outside the window of the seismic signal causes a significant decrease in the beam steer signal-to-noise ratio. The Hanning window removes this noise and allows the beam steer to identify the seismic waves.

[27] The basic beam forming method used here assumes that the waves crossing the array are planar [*Rost and Thomas*, 2002]. If the plane wave condition is not met, this method of beam forming will not work as a beam former (see *Almendros et al.* [1999] for example for an extension of beam forming to analyze circular wavefronts), but one can still use the $\vec{k} = 0$ beam stack to estimate both common mode noise and the reference stations absolute displacements, GPS multipath and noise. Using the $\vec{k} = 0$ beam stack in this manner works even if the earthquake is located within the network and for arrays with regular spacing.

5. HRGPS Displacement Time Series Model

[28] We will now examine a simple model for the HRGPS time series that takes into account two independent noise sources that affect all methods of GPS processing, review the standard methods to reduce their effects, and investigate how beam forming can compliment them. The starting

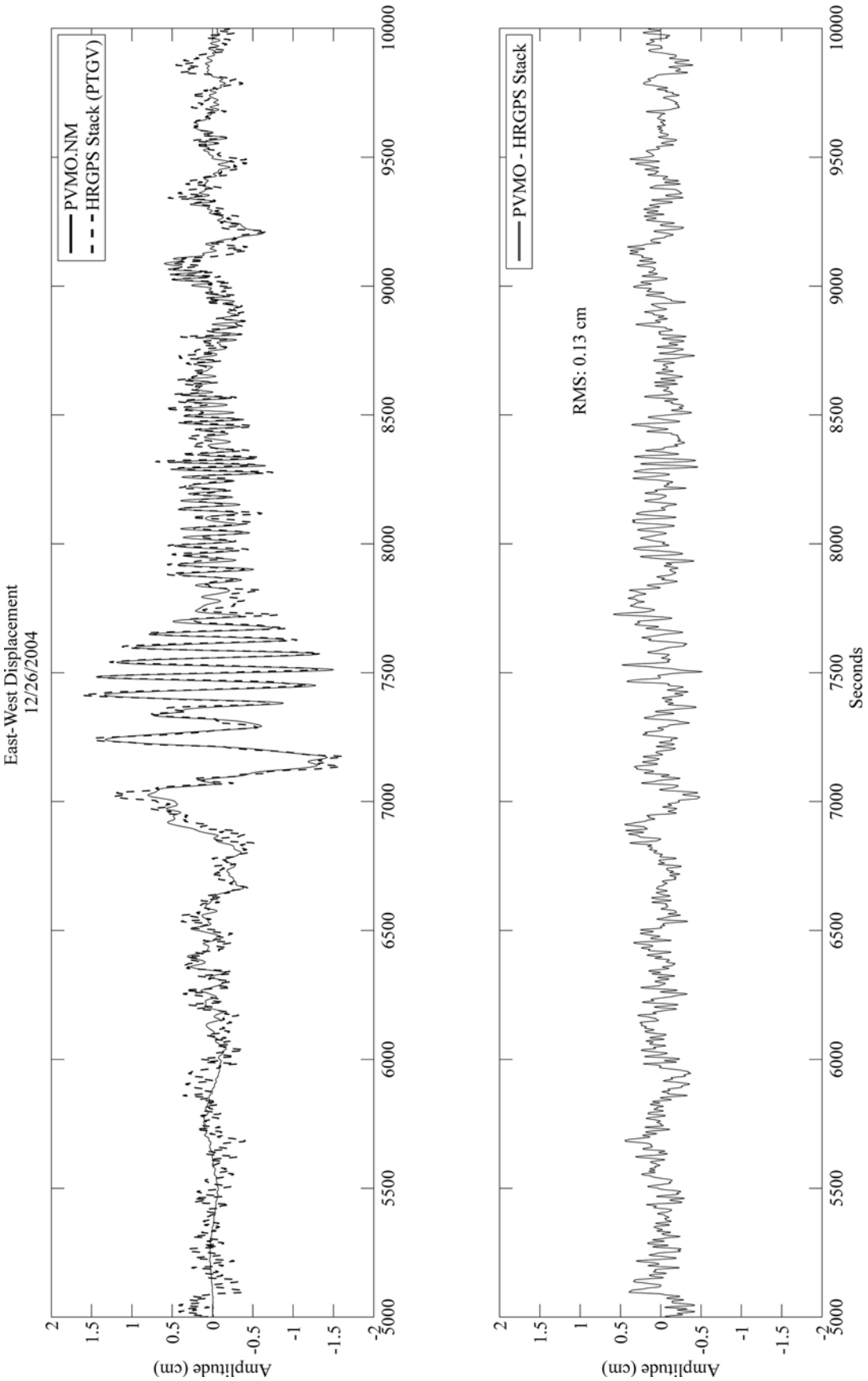

Figure 8. (top) Absolute displacements for the HRGPS station PTGV and the broadband seismometer PVMO. Both signals been band pass filtered between 0.009 and 0.08 Hz. (bottom) Difference between the two. The Hanning window is not applied to these time series.

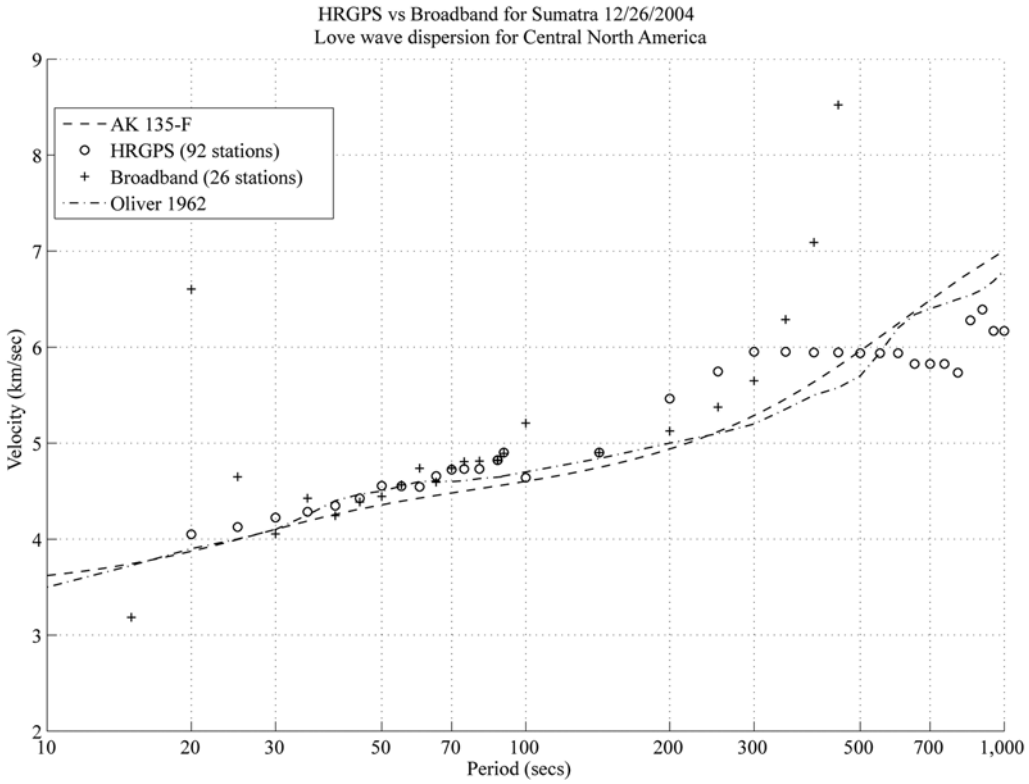

Figure 9. Measured phase velocities obtained by beam forming band-passed displacement time series for broadband seismometer data (pluses) and GPS absolute displacements (circles). An observational dispersion curve [*Oliver*, 1962] and a theoretical curve from velocity model AK135-F [*Kennett et al.*, 1995] are shown are shown by dash-dotted and dashed lines, respectively.

model for the measured absolute displacement, A, at station n is

$$A_n = D_n + N_n,$$

where D is the actual displacement and N is errors and noise. The first noise source we will examine is GPS multipath. Considering GPS multipath separately from other noise sources, the displacements at a station can be modeled as

$$A_n = D_n + M_n + N_n,$$

where M is the contribution of GPS multipath and N contains all remaining errors and noise. Since M can be estimated, it can be subtracted from the displacement estimate to produce a GPS multipath reduced displacement time series,

$$\widetilde{A}_n = A_n - \langle M_n \rangle.$$

While called filtering, this is actually superposition and not the standard signal processing use of the term filtering, which is a time domain convolution or frequency domain multiplication. We will discuss the connection between the two ideas later.

[29] Sidereal filters are usually produced by averaging over several days, which has the additional affect of low-pass filtering the estimate of $\langle M \rangle$, and *Bilich et al.* [2008] report that modified sidereal filtering works best for periods greater than 10 s. In cases where the geometry or properties of the reflectors of the GPS signal change significantly and quickly the assumption of stationarity of the GPS multipath required for sidereal filtering may be compromised sufficiently that it fails. This was the case for several stations from the Michigan HRGPS array due to a freezing rain/snow storm on the day of the Sumatra-Andaman earthquake. The affect of GPS multipath, M, is dependent on the local reflection environment at each station and is unique to each station. GPS multipath, therefore, should not be correlated between stations, and array processing can be used to test this hypothesis. In the beam steering results shown in Figure 7a, we see only two coherent waves, and each can be easily explained in terms of either seismic waves or common mode and noise not associated with seismic waves.

[30] How well beam forming works depends on whether GPS multipath or other noise is coherent. If GPS multipath is coherent, it will produce a peak or peaks that compete with those of the coherent seismic signals. Since GPS multipath is a local phenomenon, we expect it to be incoherent between stations, and, therefore, only raise the noise floor in the beam forming process. It should not generate spurious peaks. The peaks associated with the seismic waves in Figures 7a and 7b are well defined with respect to the background, and there are no other notable peaks. Beam forming of HRGPS displacement time series

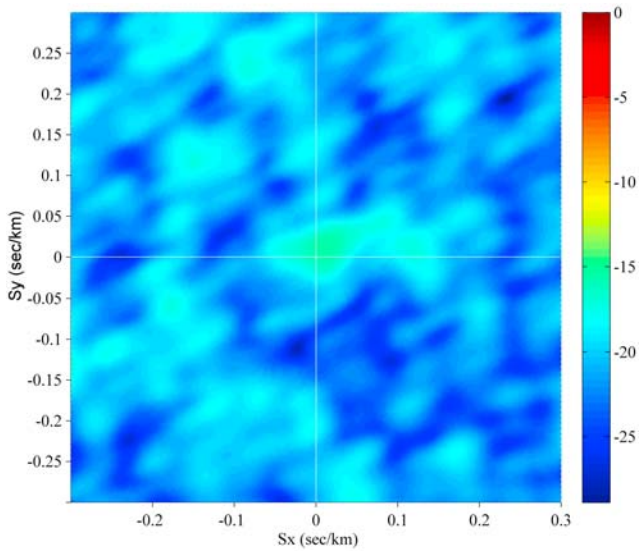

Figure 10a. Beam form results for relative displacement time series recorded during an aseismic period. The small central peak represents the nonseismic component of the common mode signal. The absence of significant peaks in the $S_x - S_y$ plane indicates there are no coherent signals crossing the array.

data for a period without seismic waves (Figures 10a and 10b) does not show the existence of coherent signals generated by GPS multipath. The effect of GPS multipath, therefore, is only an increase in the noise floor in the (k_x, k_y) plane. An important advantage of beam forming, therefore, is a reduction of the effect of GPS multipath noise in the frequency domain. Beam forming also does not rely on the assumption of sidereal stationarity of GPS multipath, so it is not susceptible to problems from a changing GPS multipath environment, such as that documented due to soil moisture variation [*Larson et al.*, 2008a, 2008b]. We purposely did not apply sidereal filtering to the HRGPS data before beam forming and observe that the beam associated with the seismic wave is well defined with respect to the noise floor in the (k_x, k_y) plane (Figures 7a and 7b) and that there is no coherent energy in the aseismic time series (Figures 10a and 10b).

[31] The second GPS noise source is common mode noise. *Wdowinski et al.* [1997] developed spatial filtering to estimate and remove common mode noise in the daily network position time series from traditional 30 s epoch data. In an analysis of the near field coseismic and post-seismic deformation associated with the 1992 Landers earthquake *Wdowinski et al.* [1997] used a stack, or average,

$$S(t) = \frac{1}{N}\sum_{n=1}^{N} A_n(t),$$

of the individual displacement time series, $A_n(t)$, to estimate the common mode noise. Comparing this to the expression for beam forming, we can see this is the expression for the $\vec{k} = 0$, or apparent velocity $v = \infty$, beam, when the $A_n(t)$ are the data used in the array processing beam forming. In the original development by *Wdowinski et al.* [1997], the daily solutions were network solutions which estimate absolute positions relative to some reference frame such as ITRF. As there is no reference or fiducial station, the stack is just the average of the absolute displacement time series, and it provides an estimate of the common mode noise.

[32] The idea of spatial filtering is to estimate a time series, S, which is common to all stations. As with sidereal filtering, since S can be estimated independently, it can be included in the model for the seismic time series,

$$A_n = D_n + M_n + S + N_n,$$

where N_n contains all the remaining, nonmodeled noise. The correction for common mode noise is a filter that is implemented using superposition. The final model for the displacement time series is

$$\approx A_n = A_n - \langle M_n \rangle - \langle S \rangle - N,$$

where the individual sidereal, $\langle M_n \rangle$, and global spatial, $\langle S \rangle$, filter estimates are independent and can be applied in any order. In the case of the spatial filter of *Wdowinski et al.* [1997], we have shown using beam forming that it is simply $1 - \delta(\vec{k})$ in the frequency domain. The effect of the filter in the time domain at each time is to subtract the average value of the network of stations at that time. The frequency domain filter operation to produce the spatial filter stack is simply $\delta(\vec{k})$ and subtracting the $\vec{k} = 0$ beam from the time series at each station implements this filter. While this method of estimating absolute displacements was developed for the case of plane waves crossing an array, it is more general and will work with any network, including one in which the earthquake is inside the network.

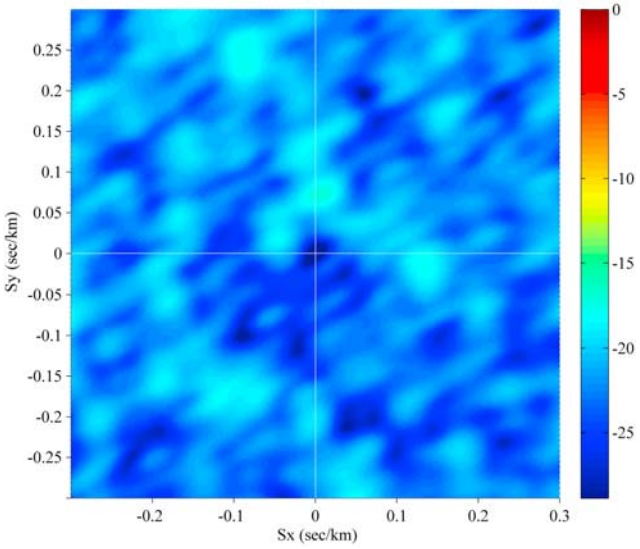

Figure 10b. Beam form results for absolute displacement time series produced by removing the $\vec{k} = 0$ beam common mode from the data in a. Note that the background noise pattern is similar to that in Figure 10a and there are no significant peaks. This indicates that multipath, which is thought to be the most significant contributor to the aseismic time series, is incoherent between stations across the array.

[33] *Larson et al.* [2007] and *Bilich et al.* [2008] applied spatial filtering to 1 Hz HRGPS relative displacement time series of the Denali earthquake. They estimated absolute seismic displacement time series at a number of HRGPS stations in the western United States at epicentral distances of 150 to 4000 km using a reference station not affected by seismic waves at 5300 km epicentral distance. A small network of three additional stations, using the same reference station, and also not being affected by the seismic waves, was used to estimate the spatial filter. This method of estimating the spatial filter potentially introduces an unknown error as the common mode noise for the data and spatial filter networks may be different [*Bilich et al.*, 2008].

[34] *Wang et al.* [2007] compared 1 Hz HRGPS data, also processed with TRACK, with accelerometer data from the epicentral region of the 2003, M 6.5, San Simeon earthquake. Following the philosophy above to produce absolute displacement time series, *Wang et al.* [2007] selected a small set of sites assumed to be outside the region affected by the seismic waves and used one of these for the reference station and the remaining ones to form the spatial filter. Surface waves, whose arrival times are consistent with the location of the reference station, are clearly observed in both the spatial filter stack and in the displacement time series of the stations in the epicentral region. Subtracting the spatial filter stack from the relative displacement time series for stations in the epicentral area removes the surface waves affecting the reference station, producing a time series that represents absolute displacements at the epicentral station only.

[35] As discussed earlier, *Bock et al.* [2004] also examined 1 Hz relative displacement time series of the Denali earthquake from a network of 4 HRGPS stations with short (<50 km) baselines in southern California using instantaneous positioning. Because this method is limited to short baselines, one of the stations, which was simultaneously affected by the seismic waves, was used as the reference. *Bock et al.* [2004] note that the three resulting HRGPS time series are therefore ''biased'' by the reference station motion, although the bias was not quantified. *Bock et al.* [2004] used the same three relative displacement time series being analyzed to estimate the spatial filter. This is the same as we have done here, but we have used a much larger number of stations. *Bock et al.* [2004] interpreted the stack to represent only the common mode noise associated with GPS processing, and not to also include the absolute displacements of the reference site. The spatial filter stack, as we have shown here however, also includes the absolute displacements of the reference station, so application of the spatial filter in this case also changed the relative displacements at the nonreference stations to absolute displacements. After the spatial filtering, the RMS differences between the integrated accelerometer data and the HRGPS data at the three nonreference stations were reduced by amounts varying between approximately 3 and 20%. In this case, in which all the sites are being equally affected by the seismic waves, it is not obvious that one of the time series is relative displacements, and the other is absolute displacements either visually or from the RMS differences.

[36] Array processing beam forming clearly shows that absolute displacement time series at the reference station can be obtained by using the $\vec{k} = 0$ beam of the array beam steer to produce the spatial filter. This observation greatly simplifies both the processing and the interpretation. It removes the constraint that the reference station is not affected by the seismic waves, and shows that it is not necessary to use an auxiliary network, also with the restriction it is not affected by the seismic waves, to estimate the common mode effects. By removing the $\vec{k} = 0$ beam common mode, the time series at the nonreference stations can now be interpreted as absolute displacement seismograms. This method also benefits statistically from the larger number of stations that contribute to the estimation of the $\vec{k} = 0$ beam common mode, especially when the assumption that the reference station is not being affected by the seismic waves is violated.

[37] We will now examine the relationship between sidereal and spatial filtering and the formal signal processing definition of filtering. Since filtering is a linear operation, one can take the difference in the time domain between a filtered and unfiltered version of the same time series to generate a new time series. An example of this is the implementation of a high pass filter by subtracting a low-pass filtered version of a signal from the original signal, which can be done in either the time or frequency domain. This implementation is given in the time domain by

$$A_{hp}(t) = A_{unfiltered}(t) - A_{lp}(t).$$

In general, the $A_{lp}(t)$ filter term is dependent on both the time series to be filtered and the properties of the filter. This is how we implement the common mode filter above, by subtracting the $\vec{k} = 0$ beam from the time series at each station. To determine $A_{filtered}(t)$ in the time domain, we convolve the signal, $A_{unfiltered}(t)$, with the filter's time domain representation, $FC(t)$,

$$A_{filtered}(t) = A_{unfiltered}(t) * FC(t) = \int_{-\infty}^{\infty} A_{unfiltered}(t-\tau)FC(\tau)d\tau.$$

To determine $A_{filtered}(t)$ using the frequency domain, we multiply the Fourier transforms of $A_{unfiltered}(t)$ and $FC(t)$ in the frequency domain and transform the resulting product back to the time domain. Whichever method we use, the filter has to be quantifiable in both the time or frequency domains.

[38] In the case of sidereal and modified sidereal filtering,

$$\widetilde{A}_{sidereallyfiltered}(t_{st}) = A_{unfiltered}(t_{st}) - M(t_{st}),$$

where t_{st} is sidereal time, assume that the $M(t_{st})$ sidereal filter term is approximately stationary and can, therefore, be estimated. If the assumption is correct, then the measured signal is the sum of a known signal, the GPS multipath, and an unknown signal, which is the desired signal. In this case, subtracting the known signal is an excellent way to obtain the unknown signal. This is especially true if the spectrum of the known signal overlaps significantly with that of the desired signal, as in this case frequency domain filtering will not be able to separate the two. Beam forming shows that GPS multipath can be separated from the seismic waves in the spatial frequency domain, i.e., GPS multipath does

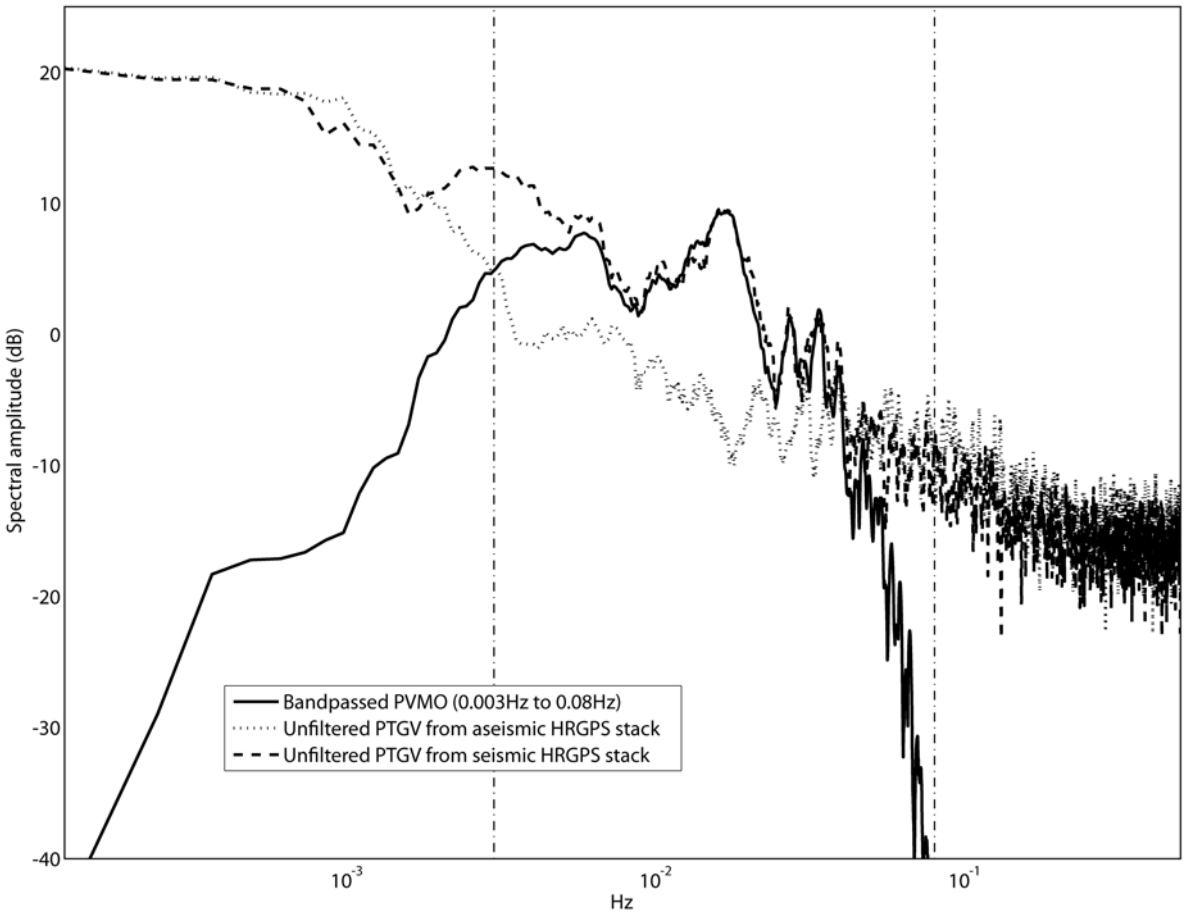

Figure 11. Power spectra of the absolute displacements of the Love wave shown in Figure 8 (top) for the broadband seismometers (black solid line) and HRGPS (gray dashed line), and aseismic HGPS multipath (and other noise) only (gray dotted line). The limits of the seismic data are due to the decrease in sensitivity of the broadband seismometer at periods greater than 300 s and a low-pass filter with a corner at 12.5 s.

not significantly overlap in spatial frequency with the signal, so we can use array processing to remove GPS multipath in the frequency domain.

[39] To use array processing to implement GPS multipath filtering, a simple filter can be constructed in the frequency domain using a set of curves containing the coherent waves and inside of which the weight is 1, while outside these curves the weight is zero. One then multiplies this filter with the Fourier transform of the signal in the frequency domain and inverse transforms back to the time domain to obtain multipath reduced time series. One could also compute $1 - filter$ in the frequency domain, multiply it by the Fourier transform of the signal, inverse transform this to the time domain to generate the GPS multipath time series, and subtract this from the original time series. This looks like sidereal filtering in that we are subtracting two time domain signals, but the GPS multipath time series produced using the spatial frequency domain method is the measured instantaneous multipath, which should be similar to the multipath time series used in the sidereal filter if the stationarity assumption of sidereal filtering is valid. In either case we obtain a time series with the noncoherent part of the GPS multipath at each station removed. The spatial frequency domain based method will not remove the contribution of multipath that is inside the $f - \vec{k}$ passband for the seismic waves. The filtering process is straightforward for uniformly sampled data where we can use the FFT but is more difficult for nonuniformly or randomly sampled data where the frequency domain representation is not unique and efficient computational tools such as the FFT do not exist.

[40] We are developing techniques for the non uniform array based on frequency wave number filtering to return data filtered in the frequency domain to GPS multipath reduced data in the time domain. Beam forming, which is easy to compute for any array, can also be used to design the filter. Unfortunately beam forming can only determine the magnitude, not the phase, in the frequency domain, so it cannot be used in the inverse Fourier transform. Removing GPS multipath using $f - \vec{k}$ filtering is not completely general as it depends on the beam forming model in which plane waves cross an array. If the earthquake occurs inside the network or the wavefronts have significant curvature, simple $f - \vec{k}$ filtering does not work.

[41] Figure 11 shows the power spectra of absolute displacements for the earthquake and from an aseismic

day, one of the days used to generate the sidereal filter, from the colocated HRGPS (PTGV) and broadband (PVMO) stations. The HRGPS time series for PTGV represent the absolute displacements of the reference site from the $\vec{k} = 0$ beam or spatial filtering stack. As reported by *Bilich et al.* [2008], but over a narrower frequency band, the HRGPS noise floor is much higher than that for the broadband seismometer data, but the two power spectra for the earthquake data agree well from 0.002 to 0.04 Hz where significant energy is seen in both spectra above their noise floors. Comparison of the seismic and aseismic power spectra suggests that the proposal of a dynamic cancellation of GPS multipath during seismic shaking by *Bock et al.* [2004] is unnecessary. If such a dynamic cancellation occurred, then GPS multipath would be reduced or removed during the passage of the seismic waves. Sidereal filtering would, therefore, be unnecessary during that time, and application of sidereal filtering would insert the dynamically canceled GPS multipath back into the time series. As with the case above, where it is not possible to distinguish absolute from relative displacement HRGPS time series when comparing them to absolute displacement seismic data, it is not generally possible to see the effects of multipath on the seismic time series when the seismic waves are well above the noise.

[42] The Sumatra-Andaman earthquake also generated large amplitude Rayleigh waves. The N-S azimuth to CNA is close to nodal for Rayleigh waves, however, and the Rayleigh waves are smaller than the Love waves. Using beam forming we were able to detect, but not fully analyze, Rayleigh waves on the radial horizontal component (north-south), but not on the vertical, component. This is not surprising as GPS is less precise, by a factor of 3–5, in the vertical.

6. Conclusions

[43] We have shown HRGPS displacement time series can be used to produce surface wave dispersion curves that compare very well with those produced by broadband seismometers. We have also used beam steering to show that the differential displacement time series can be simply modeled as the difference of the absolute motions of the reference and kinematic stations. Using the relative displacements of all the kinematic stations to form the spatial filter, which is the $\vec{k} = 0$ beam of beam forming, we obtain estimates of the absolute displacement, multipath, and noise of the reference station plus the GPS common mode noise. When this $\vec{k} = 0$ beam or spatial filter time series is subtracted from the kinematic time series, we obtain absolute displacement time series with the common mode, which contains common mode noise plus the reference station contribution, removed. Using the $\vec{k} = 0$ beam allows estimation of absolute displacement time series whether or not the reference station is being affected by seismic waves. Array processing also does not require processing of a second network of stations unaffected by the seismic waves to estimate the common mode noise. By using all the data available, rather than a handful of distant stations, the array processing $\vec{k} = 0$ beam produces a better estimation of the common mode filter as uncorrelated noise is reduced by a factor of $\sqrt{N}$, where N is the number of stations. The absolute time series of the reference station, which also contains the common mode noise, can be included in the beam steer of the absolute displacement time series. This would have a negligible effect on the results of the beam steer with almost 100 stations, but would allow for both multipath and common mode noise removal from the reference station time series by the $f - \vec{k}$ filtering.

[44] For large amplitude displacements at long and very long periods at teleseismic distances, or associated with high accelerations in the epicentral region, HRGPS can provide an important, and due to the large number of HRGPS stations, dense seismic wavefield sampling that complements traditional seismic data. For the largest signals produced by earthquakes, GPS data are also less susceptible to clipping than broadband seismometers, although as mentioned earlier, the question of preventing temporally aliased recording in the epicentral region has not yet been properly addressed. Other advantages of GPS are that it produces an estimate of displacement directly and does not have to be integrated once or twice from velocity or acceleration respectively as with broadband seismometer or accelerometer data and that the response continues to longer periods than seismometers. Our preliminary analysis indicates application of frequency wave number $(f - \vec{k})$ filtering can provide a GPS multipath reduction method that will complement sidereal filtering, and we are currently working on implementation of $f - k$ filtering for nonuniform or random arrays. GPS multipath and common mode noise reduced, absolute displacement seismograms will facilitate using HRGPS seismograms for a wide range of traditional seismic applications, especially slip inversion and estimation of strong motion in the region suffering permanent coseismic displacements.

[45] **Acknowledgments.** The seismic data were obtained from the ANSS Cooperative New Madrid Seismic Network and the 1 Hz HRGPS data from the Michigan, N. Carolina, and Ohio state reference networks, the DOT FAA WASS and CORS networks, and the MAEC GAMA network. This work was supported in part by the Mid-America Earthquake Center (MAEC), an Earthquake Engineering Research Center of the NSF, under award EEC-9701785. We thank T. Herring, an anonymous reviewer, and the Associate Editor for constructive reviews.

References

King, R. W., and Y. Bock (2000), Documentation for the GAMIT GPS analysis software, Dep. of Earth and Planet. Sci., Mass. Inst. of Technol., Cambridge.

Almendros, J., J. M. Ibáñez, G. Alguacil, and E. Del Pezzo (1999), Array analysis using circular-wave-front geometry: An application to locate the nearby seismo-volcanic source, *Geophys. J. Int.*, *136*, 159–170, doi:10.1046/j.1365-246X.1999.00699.x.

Bilich, A., J. F. Cassidy, K. M. Larson, and G. P. S. Seismology (2008), Application to the 2002 M_w 7.9 Denali Fault earthquake, *Bull. Seismol. Soc. Am.*, *98*(2), 593–606, doi:10.1785/0120070096.

Bock, Y., S. A. Gourevitch, C. C. Councelman, R. W. King, and R. I. Abbot (1986), Interferometric analysis of GPS phase observations, *Manuscr. Geod.*, *11*, 282–288.

Bock, Y., R. M. Nikolaidis, P. J. de Jonge, and M. Bevis (2000), Instantaneous geodetic positioning at medium distances with the Global Positioning System, *J. Geophys. Res.*, *105*(B12), 28,223–28,253, doi:10.1029/2000JB900268.

Bock, Y., L. Prawirodirdjo, and T. I. Melbourne (2004), Detection of arbitrarily large dynamic ground motions with a dense high-rate GPS network, *Geophys. Res. Lett.*, *31*, L06604, doi:10.1029/2003GL019150.

Brooks, B. A., M. Bevis, R. Smalley Jr., E. Kendrick, R. Manceda, E. Lauría, R. Maturana, and M. Araujo (2003), Crustal motion in the southern Andes (26°–36°S): Do the Andes behave like a microplate?, *Geochem. Geophys. Geosyst.*, *4*(10), 1085, doi:10.1029/2003GC000505.

Brune, J. N., J. E. Nafe, and J. E. Oliver (1960), A simplified method for the analysis and synthesis of dispersed wave trains, *J. Geophys. Res.*, *65*(1), 287–304, doi:10.1029/JZ065i001p00287.

Burg, J. P. (1964), Three-dimensional filtering with an array of seismometers, *Geophysics*, *29*, 693–713, doi:10.1190/1.1439406.

Burr, E. J. (1955), Sharpening of observational data in two dimensions, *Aust. J. Phys.*, *8*, 30–53.

Capon, R. (1969), High-resolution frequency-wavenumber spectrum analysis, *Proc. IEEE*, *57*, 1408–1418, doi:10.1109/PROC.1969.7278.

Capon, R., R. J. Greenfield, and R. J. Kolker (1967), Multidimensional maximum-likelihood processing of a large aperture seismic array, *Proc. IEEE*, *55*, 192–211, doi:10.1109/PROC.1967.5439.

Chen, G. (1998), GPS kinematics positioning for the Airborne Laser Altimetry at Long Valley, California, Ph.D. thesis, 173 pp., Mass. Inst. of Technol., Cambridge.

Choi, K., A. Bilich, K. M. Larson, and P. Axelrad (2004), Modified sidereal filtering: Implications for high-rate GPS positioning, *Geophys. Res. Lett.*, *31*, L22608, doi:10.1029/2004GL021621.

Dragert, H., K. Wang, and T. S. James (2001), A silent slip event on the deeper Cascadia subduction interface, *Science*, *292*, 1525–1528, doi:10.1126/science.1060152.

Emore, G., J. Haase, K. Choi, K. M. Larson, and A. Yamagiwa (2007), Recovering absolute seismic displacements through combined use of 1-Hz GPS and strong motion accelerometers, *Bull. Seismol. Soc. Am.*, *97*(2), 357–378, doi:10.1785/0120060153.

Frosch, R. A., and P. E. Green Jr. (1966), The concept of a large aperture seismic array, *Proc. R. Soc. London, Ser. A*, *290*(1422), 368–384, doi:10.1098/rspa.1966.0056.

Gangi, A. F., and D. Disher (1968), A space-time filter for seismic models, *Geophysics*, *33*, 88–104, doi:10.1190/1.1439923.

Genrich, J. F., and Y. Bock (1992), Rapid resolution of crustal motion at short ranges with the Global Positioning System, *J. Geophys. Res.*, *97*(B3), 3261–3269, doi:10.1029/91JB02997.

Green, P. E., R. A. Frosch, and C. F. Romney (1965), Principles of an experimental Large Aperture Seismic Array (LASA), *Proc. IEEE*, *53*, 1821–1833, doi:10.1109/PROC.1965.4453.

Hatanaka, Y., T. Hiromichi, A. Yoshiaki, Y. Iimura, K. Kobayashi, and H. Morishita (1994), Coseismic crustal displacements from the 1994 Hokkaido-Toho-Oki earthquake revealed by a nationwide continuous GPS array in Japan—Results of GPS kinematic analysis, paper presented at Japanese Symposium on GPS, Natl. Comm. for Geod., Sci. Counc. of Jpn., GPS Consortium of Jpn., Tokyo.

Herring, T. A. (2009a), Documentation of the GLOBK software version 10.35, Mass. Inst. of Technol., Cambridge.

Herring, T. A. (2009b), TRACK GPS kinematic positioning program, version 1.21, Mass. Inst. of Technol., Cambridge.

Herring, T. A. (2009c), Example of the usage of TRACK, Massachusetts's Institute Mass., Inst. of Technol., Cambridge. (Available at http://geoweb.mit.edu/~tah/track_example/)

Holm, S., B. Elgetun, and G. Dahl (1997), Properties of the beampattern of weight- and layout-optimized sparse arrays, *IEEE Trans. Ultrason. Ferroelectr. Frequation Control*, *44*, 983–991, doi:10.1109/58.655623.

Hudnut, K. W., et al. (1994), Co-seismic displacements of the 1992 Landers earthquake sequences, *Bull. Seismol. Soc. Am.*, *84*, 625–645.

Ji, C., K. M. Larson, Y. Tan, K. W. Hudnut, and K. Choi (2004), Slip history of the 2003 San Simeon earthquake constrained by combining 1-Hz GPS, strong motion, and teleseismic data, *Geophys. Res. Lett.*, *31*, L17608, doi:10.1029/2004GL020448.

Kanasewich, E. R., C. D. Hemmings, and T. Alpaslan (1973), Nth-root stack nonlinear multichannel filter, *Geophysics*, *38*, 327–338, doi:10.1190/1.1440343.

Kennett, B. L. N., E. R. Engdahl, and R. Buland (1995), Constraints on seismic velocities in the Earth from travel times, *Geophys. J. Int.*, *122*, 108–124, doi:10.1111/j.1365-246X.1995.tb03540.x.

Kobayshi, R., S. Miyazaki, and K. Koketsu (2006), Source processes of the 2005 west off Fukuoka Prefecture earthquake and its largest aftershock inferred from strong motion and 1-Hz GPS data, *Earth Planets Space*, *58*, 57–62.

Kouba, J. (2003), Measuring seismic waves induced by large earthquakes with GPS, *Stud. Geophys. Geod.*, *47*, 741–755, doi:10.1023/A:1026390618355.

Kreemer, C., W. E. Holt, and A. J. Haines (2003), An integrated global model of present-day plate motions and plate boundary deformation, *Geophys. J. Int.*, *154*, 8–34, doi:10.1046/j.1365-246X.2003.01917.x.

Kreemer, C., G. Blewitt, W. C. Hammond, and H.-P. Plag (2006), Global deformation from the great 2004 Sumatra-Andaman earthquake observed by GPS: Implications for rupture process and global reference frame, *Earth Planets Space*, *58*, 141–148.

Larson, K., P. Bodin, and J. Gomberg (2003), Using 1-Hz GPS data to measure deformations caused by the Denali Fault earthquake, *Science*, *300*, 1421–1424, doi:10.1126/science.1084531.

Larson, K. M., A. Bilich, and P. Axelrad (2007), Improving the precision of high-rate GPS, *J. Geophys. Res.*, *112*, B05422, doi:10.1029/2006JB004367.

Larson, K. M., E. E. Small, E. Gutmann, A. L. Bilich, J. Braun, and V. Zavorotny (2008a), GPS as a soil moisture sensor, *Eos Trans. AGU*, *89*(53), Fall Meet. Suppl., Abstract G41D-08.

Larson, K. M., E. E. Small, E. Gutmann, A. Bilich, P. Axelrad, and J. Braun (2008b), Using GPS multipath to measure soil moisture fluctuations: Initial results, *GPS Solut.*, *12*(3), 173–177, doi:10.1007/s10291-007-0076-6.

Miyazaki, S., K. M. Larson, K. Choi, K. Hikima, K. Koketsu, P. Bodin, J. Haase, G. Emore, and A. Yamagiwa (2004), Modeling the rupture process of the 2003 September 25 Tokachi-Oki (Hokkaido) earthquake using 1-Hz GPS data, *Geophys. Res. Lett.*, *31*, L21603, doi:10.1029/2004GL021457.

Nafe, J. E., and J. N. Brune (1960), Observations of phase velocity for Rayleigh waves in the period range 100 to 400 seconds, *Bull. Seismol. Soc. Am.*, *50*(3), 427–439.

Nikolaidis, R., Y. Bock, P. J. de Jonge, P. Shearer, D. C. Agnew, and M. Van Domselaar (2001), Seismic wave observations with the Global Positioning System, *J. Geophys. Res.*, *106*, 21,897–21,916, doi:10.1029/2001JB000329.

Ohta, Y., J. Freymueller, S. Hreinsdóttir, and H. Suito (2006), A large slow slip event and the depth of the seismogenic zone in the south central Alaska subduction zone, *Earth Planet. Sci. Lett.*, *247*, 108–116, doi:10.1016/j.epsl.2006.05.013.

Oliver, J. (1962), A summary of observed seismic surface wave dispersion, *Bull. Seismol. Soc. Am.*, *52*(1), 81–86.

Rost, S., and C. Thomas (2002), Array Seismology: Methods and Applications, *Rev. Geophys.*, *40*(3), 1008, doi:10.1029/2000RG000100.

Sella, G. F., T. H. Dixon, and A. Mao (2002), REVEL: A model for Recent plate velocities from space geodesy, *J. Geophys. Res.*, *107*(B4), 2081, doi:10.1029/2000JB000033.

Takasu, T. (2006), High-rate precise point positioning: Observation of crustal deformation by using 1-Hz GPS data, paper presented at GPS/GNSS Symposium 2006, Tokyo Univ. of Mar. Sci. and Technol., Tokyo, 15–17 Nov.

vanDam, T., G. Blewitt, and M. B. Heflin (1994a), Atmospheric pressure loading effects on Global Positioning System coordinate determinations, *J. Geophys. Res.*, *99*(B12), 23,939–23,950, doi:10.1029/94JB02122.

vanDam, T., G. Mader, and M. Schenewerk (1994b), GPS detects coseismic and post-seismic surface displacements caused by the Northridge earthquake, *Eos Trans. AGU*, *75*(16), Spring Meet. Suppl., 103.

Wang, G.-Q., D. M. Boore, G. Tang, and X. Zhou (2007), Comparisons of ground motions from collocated and closely spaced one-sample-per-second Global Positioning System and accelerograph recordings of the 2003 M 6.5 San Simeon, California, earthquake in the Parkfield region, *Bull. Seismol. Soc. Am.*, *97*(1B), 76–90, doi:10.1785/0120060053.

Wdowinski, S., Y. Bock, J. Zhang, P. Fang, and J. Genrich (1997), Southern California permanent GPS geodetic array: Spatial filtering of daily positions for estimating coseismic and postseismic displacements induced by the 1992 Landers earthquake, *J. Geophys. Res.*, *102*, 18,057–18,070, doi:10.1029/97JB01378.

Whiteway, F. E. (1966), The use of arrays for earthquake seismology, *Proc. R. Soc. London, Ser. A*, *290*(1422), 328–342, doi:10.1098/rspa.1966.0054.

J. P. Davis and R. Smalley Jr., Center for Earthquake Research and Information, University of Memphis, 3876 Central Avenue, Suite 1, Memphis, TN 38152-3050, USA. (rsmalley@memphis.edu)